

1 CRISPR-LRS for mapping transgenes in the mouse genome

2

3

4 W. Bart Bryant*, Allison Yang, Susan Griffin, Wei Zhang, Xiaochun Long, and Joseph M. Miano*

5 Department of Medicine and Vascular Biology Center. Medical College of Georgia at Augusta

6 University; Augusta, GA 30912

7

8

9 * corresponding authors (WILBRYANT@augusta.edu and jmiano@augusta.edu)

10

11

12

13

14 **Abstract**

15 Microinjected transgenes, including bacterial artificial chromosomes (BACs), insert randomly in
16 the mouse genome. Traditional methods of mapping a transgene are challenging, thus
17 complicating breeding strategies and the accurate interpretation of phenotypes, particularly
18 when a transgene disrupts critical coding or noncoding sequences. Here, we introduce
19 CRISPR-Cas9 long-read sequencing (CRISPR-LRS) to ascertain transgene integration locus
20 and estimated copy number. This method revealed integration loci for both a BAC and *Cre*-
21 driver line, and estimated the copy numbers for two other BAC mouse lines. CRISPR-LRS
22 offers an easy approach to establish robust breeding practices and accurate phenotyping of
23 most any transgenic mouse line.

24

25

26

27 Despite the routine use of transgenic mice, greater than 90% of transgenic alleles in the
28 Mouse Genome Database have yet to be mapped (1, 2) even though it is broadly accepted that
29 random integration of a transgene can disrupt coding exons and functional noncoding
30 sequences (eg, enhancer, long noncoding RNA), thus complicating data interpretation.
31 Fluorescence in situ hybridization (FISH) can map a transgene to a chromosomal band, but
32 lacks nucleotide resolution (3). Hybridization, targeted locus amplification (TLA), and linear
33 amplification-mediated PCR (LAM-PCR), rely on short-read sequencing and cannot resolve
34 complex genome inversions/deletions (4-7). Inverse PCR has high failure rates due to
35 concatemerization of most transgenes (8). Recently, whole genome sequencing (WGS) with
36 long-read sequencing platforms, PacBio or Oxford Nanopore Technologies (ONT), have been
37 used to map transgenes (2, 9). However, even with ~7.5Gb of sequencing data for ~3x
38 coverage of the mouse genome, researchers cannot be assured to find reads that identify the
39 breakpoint of the transgene.

40 We propose a more targeted approach to map a transgene by combining (i) the RNA
41 programmable CRISPR-Cas9 system (10) and (ii) long-read length coverage of the ONT
42 sequencing platform (11, 12). Previous studies have combined CRISPR-Cas9 with LRS to
43 enrich for genomic elements (13-20); however, no studies until now have combined CRISPR
44 and LRS to map transgenes in an animal model. CRISPR-LRS can be designed (i) to target a
45 genomic section (Targeted-CRISPR-LRS) or (ii) to enrich genomic sections (Enrichment-
46 CRISPR-LRS). In this study, CRISPR-LRS successfully mapped a single-copy BAC and a multi-
47 copy *Cre* in the mouse genome. CRISPR-LRS represents a facile tool for mapping transgenes
48 in experimental animal models, thus informing investigators as to best breeding practices and
49 potential genetic confounders.

50

51 **Results/Discussion**

52

53 For the four transgenic mouse lines in this study, seven CRISPR-LRS libraries (Targeted
54 or Enrichment) were sequenced with the minION platform for a total of ~1.8Gb at ~400,000
55 reads (see Supp. Table 1 and 2). Reads mapped to their corresponding reference sequence
56 with a range of 0.02% - 0.52% (Supp. Table 2) and will be referred to as informative long-reads
57 below.

58

59

60

61 **CRISPR-LRS mapping of BAC mouse lines**

62 The mouse line carrying the RP11-744N12 BAC was generated to study human-specific
63 long noncoding RNA, *SENCR* (21). To map where this 217 kb BAC integrated into the mouse
64 genome, two Targeted-CRISPR-LRS libraries were made 5 kb or 3 kb from the 5' and 3' ends of
65 each BAC sequence, respectively (Figure 1A, Supp. Fig 1i, and Supp. Table 1). Both libraries
66 yielded 0.03% of reads (0.9 kb – 25 kb) that mapped to the reference sequence (Figure 1Ai and
67 Supp. Table 2). Notably, manual inspection of informative long-reads revealed ~7 kb of
68 pBACe3.6 vector sequence accompanying transgene and mouse chromosome 15 sequences
69 (Figure 1Ai). Further, informative long-reads over 6 kb for 5' end and 10 kb for 3' end, found
70 RP11-744N12 integrated within the first intron of *Egflam* (Chr15:7,344,678; GRCm38/mm10)
71 (Figure 1A). CRISPR-LRS also mapped mouse BAC lines, CTD-2518N7 and RP11-997L11,
72 and found informative long-reads with the BAC-cloning vector flanked by 5' and 3' human
73 sequence, indicating integration of at least two copies of each transgenic line (Supp. Fig 1ii and
74 Supp. Fig 2).

75 While Targeted-CRISPR-LRS mapped the RP11-744N12 BAC integration locus, only a
76 few long-reads covered the integration loci. Enrichment-CRISPR-LRS queried 7.7 kb and 10.0
77 kb for the 5' and 3' terminal ends, respectively, with crRNAs enriching for (i) mouse
78 chromosome 15, (ii) pBACe3.6 cloning vector, and (iii) RP11-744N12 sequences (Figure 1Aii
79 and Supp. Fig 1iv). With 5- and 12- fold enrichment of informative reads at the 5'- and 3'-
80 terminal ends, respectively (compare Figure 1Ai to 1Aii), Enrichment-CRISPR-LRS validated the
81 Targeted-CRISPR-LRS mapping data (Figure 1Aii). Further, Sanger sequencing confirmed the
82 breakpoint of RP11-744N12 BAC and chromosome 15, within the first intron of *Egflam* (Figure
83 1Aiii and Supp. Table 1

84 Genotyping pups from a (+/tg) x (+/tg) cross with primers spanning (i) transgene and
85 chromosome 15 breakpoint and (ii) wild type chromosome 15 loci (Figure 1B), revealed near
86 Mendelian ratio: (+/tg), 17/41 at 41%; (+/+), 9/41 at 22%; (tg/tg), 15/41 at 37%. Notably, the
87 BAC transgene exists as a single copy with no loss of mouse genomic sequence at the site of
88 integration and healthy, homozygous transgenic mice indicate the absence of overt pathology.

89 While CRISPR-LRS mapped RP11-744N12 as a single copy, we wanted to check for the
90 possibility of additional integration sites as one study reported multiple integration loci for ~10%
91 of their EGFP-reporter lines by FISH (3). To verify a single integration locus, heterozygous (+/tg)
92 pups were crossed and progeny genotypes were assessed with BAC-specific primers, (Figure
93 1B). As expected, BAC-specific amplicons were present in (+/tg) and (tg/tg) pups (Figure 1B).
94 However, if a wild type (+/+) pup from the heterozygous cross exhibited BAC-specific

95 amplicons, then this result would indicate that CRISPR-LRS missed additional transgene
96 integration sites. Notably, wild type (+/+) pups from the (+/tg) x (+/tg) did not exhibit BAC-
97 specific amplicon products (Figure 1B), demonstrating CRISPR-LRS did successfully map the
98 RP11-744N12 BAC as a single copy transgenic mouse line.

99 Fortuitously, as all BAC transgenes were flanked with BAC-cloning vector sequence
100 (Figure 1 and Supp. Fig 2), copy number quantification was possible. qPCR, routine for copy
101 number variation analysis (1, 2, 5, 9), targeted the *chloramphenicol resistance gene*, a common
102 gene within BAC-vectors. With a single integration (Figure 1), (+/tg) and (tg/tg) RP11744N12
103 pups were queried by qPCR finding one and two BAC transgene copies, respectively (Supp. Fig
104 3A). As the other BAC-lines exhibited tandem integrations, only (+/tg) pups were queried, with
105 qPCR showing ~2-3 copies for both lines. Collectively, qPCR was consistent with the CRISPR-
106 LRS mapping data (Figure 1, Supp. Fig1 i and ii, Supp. Fig 2, and Supp. Fig 3A).

107

108 **CRISPR-LRS mapping of *Cre*-driver mouse line**

109 Most small transgenes lack a mapped integration locus and can possess dozens of
110 copies of the transgene, as well as complex rearrangements of the host genome (1, 2, 22). We
111 next applied CRISPR-LRS to map *Sm22-Cre*, a mouse line used to excise floxed DNA
112 sequences in early embryonic heart and smooth muscle cell-containing tissues (23). To map the
113 BAC lines, CRISPR-LRS targeted at least 2 kb from terminal ends of the transgene (Figure 1,
114 Supp. Fig 1i-ii, and Supp. Fig 2). However, because *Cre* is significantly smaller than a BAC, a
115 different Targeted-CRISPR-LRS approach was used. Specifically, two independent libraries
116 targeting 0.8 kb or 0.5 kb from the 5' and 3' end, respectively, were run on one flow cell (Figure
117 2Ai, Supp. Fig 1iii, and Supp. Table 1). At 0.52%, the *Sm22-Cre* libraries contained more
118 informative long-reads over the BAC libraries (Figure 1, Figure 2Ai, Supp. Fig 2, and Supp.
119 Table 2). Manual interrogation and alignment of >6 kb informative long-reads elucidated a mini-
120 tiled *Cre* transgene integration map consisting of multiple copies of *Cre* and genomic inversions
121 (Figure 2Ai). Three informative long-reads revealed a breakpoint between one of the *Cre*
122 transgenes and 91,527,881bp on chromosome 14 (GRCm38/mm10) (Figure 2Ai, dashed black
123 line box). Sanger sequencing verified the *Cre* and host chromosome breakpoint (Figure 2Aii and
124 Supp. Table 1).

125 Genotyping pups from a (+/tg) x (+/tg) cross with primers spanning (i) the breakpoint of
126 *Cre* and chromosome 14 and (ii) wild type chromosome 14 loci (Figure 2B), revealed near
127 Mendelian ratio: (+/tg), 20/41 at 49%; (+/+), 8/41 at 19%; (tg/tg), 13/41 at 32%.

128 To check for additional integration loci for the *Cre*-driver, heterozygous pups were
129 crossed and progeny genotypes assessed with *Cre*-specific primers, D and E (Figure 2B). Both
130 (+/tg) and (tg/tg) pups yielded amplicon products for the internal *Cre* primers, as expected
131 (Figure 2B). Notably, wild type pups from the (+/tg) x (+/tg) cross did not yield *Cre*-specific
132 amplicon products (Figure 2B), demonstrating CRISPR-LRS successfully mapped one
133 integration locus for the *Sm22Cre* mouse line.

134 As small transgenes typically integrate as concatemers (1, 2), our mini-tiled integration
135 map for *Sm22Cre* could not firmly establish copy number (Figure 2A). To address this limitation,
136 qPCR determined the copy number for the line with ~20 and ~40 copies of *Cre* for (+/tg) and
137 (tg/tg) pups, respectively (Figure 2Aiii and Supp. Figure 3B). As the *Sm22Cre* mouse has ~20
138 copies of *Cre* per allele, there were more Cas9-ribonucleoprotein (RNP) targets to cleave
139 compared to the BAC lines, explaining how the *Sm22Cre*-CRISPR-LRS libraries contained
140 more informative mapped long-reads over the BAC-CRISPR-LRS libraries (Figure 1, Figure 2,
141 Supp. Fig 2, Supp. Fig 3, and Supp. Table 2).

142

143 **Conclusions**

144

145 There are several benefits of mapping transgenes in animal models such as mice. First,
146 mapping allows investigators to accelerate the generation of desired outcomes in a complex
147 breeding scheme, (e.g., floxed alleles with *Cre*-driver lines). Second, it enables quality design of
148 genotyping assays for colony maintenance and zygosity determination. Lastly, and arguably
149 most important, it alerts one to confounding genetics caused by insertion of the transgene in a
150 coding/noncoding sequence or regulatory element (1, 2, 5, 9, 22).

151 Of the available strategies to map transgenes, WGS (2, 9) and TLA (1, 5) have the most
152 traction. However with WGS, most of the sequence data is uninformative and sequence depth is
153 substantial with ~2-5x coverage of the host genome (2, 9). Here, with only ~1.8Gb of cumulative
154 sequence data, CRISPR-LRS mapped four mouse lines with two lines yielding PCR validated
155 chromosome coordinates. TLA can be technically challenging for most labs as (i) it has
156 numerous steps; crosslinking, fragmentation, re-ligation, and amplification, and (ii) analysis can
157 require extensive computational expertise due to the nature of these fragmented sequence
158 libraries (1, 5). CRISPR-LRS (i) has less steps; Cas9 cleavage and adaptor ligation, and (ii) only
159 requires mapping long-reads with an open source tool, minimap2 (24). We envision CRISPR-
160 LRS as the 'go-to' method of mapping transgenes in any organism with a reference genome.

161 **Methods**

162

163 **Transgenic mice**

164 The *SENCR* BAC and *Sm22Cre* mouse lines were reported previously (21), (23). The human
165 CTD-2518N7 and RP11-997L11 BAC transgenic lines were generated by Cyagen
166 (www.cyagen.com) using strain C57BL/6J. All mice were maintained on strain C57BL/6J
167 through repeated back-crossing, refreshing the breeders every 5 generations to mitigate genetic
168 drift. Mouse experiments were approved by Medical College of Georgia at Augusta University
169 Institutional Animal Care and Use Committee (approval numbers 2019-1000 and 2019-0999).

170

171 **Long-read library preparation**

172 Genomic DNA (gDNA) was isolated from mouse liver tissue using Qiagen DNeasy Blood &
173 Tissue Kit (cat#69504) following manufacturer's instructions (www.qiagen.com). To limit
174 shearing of gDNA, wide bore pipette tips were used. Libraries (5µg gDNA) were prepared for
175 four different transgenic mouse lines following manufacturer's instructions for Cas9 sequencing
176 kit (SQK-CS9109) using the long fragment buffer option during library prep clean-up for seven
177 total CRISPR-LRS libraries (www.nanoporetech.com). crRNAs were designed using
178 CHOPCHOP (25) with default parameters (Supp. Table I) (<https://chopchop.cbu.uib.no>).
179 Following suggestions from ONT, all crRNAs, tracrRNA, and HiFi Cas9 were ordered from IDT
180 (www.idt.dna.com). To ensure adequate read length needed to accurately map transgene
181 integration loci, crRNAs were designed to target within 5 kb of the terminal 5' and 3' ends of the
182 BAC sequence. Further, a Targeted- or an Enrichment- CRISPR-LRS approach was performed
183 for each mouse line (see Supp. Fig. 1 for flow chart). For Targeted-CRISPR-LRS, crRNAs were
184 designed at the 5' and 3' ends of the transgene where RNPs were loaded with either one or
185 multiple crRNAs (Supp. Figure 1i - iii and Supp. Table 1). For Enrichment-CRISPR-LRS,
186 tandem crRNAs were designed up- and down- stream of the genomic region of interest (ROI)
187 and loaded onto one RNP (14, 20) (Supp. Figure 1iv and Supp. Table 1). For both approaches,
188 pre-existing DNA ends were dephosphorylated before Cas9-cutting, which yielded preferential
189 ligation of nanopore adaptors to fresh Cas9 cleavage sites as a means to target specific
190 genomic ROIs. For the RP11-744N12 BAC mouse line, two crRNAs, one targeting the 5' and
191 one targeting the 3' end of the BAC sequence, were loaded onto two separate RNPs for two
192 independent libraries (Supp. Fig. 1i). Since an integration locus for the RP11-744N12 BAC
193 mouse line was determined, Enrichment-CRISPR-LRS was further performed following

194 manufacturer's instructions (SQK-CS9109) (www.nanoporetech.com). Both 5' and 3' integration
195 loci were probed with four crRNAs loaded onto one RNP (Supp. Fig. 1iv). For the remaining
196 BAC mouse lines, CTD-2518N7 and RP11-997L11, two crRNAs were loaded onto one RNP for
197 one Cas9 library run (Supp. Fig. 1ii). For the *Cre*-driver mouse line, overlapping crRNAs
198 targeting *Cre* were designed at least 0.5 kb from 5' or 3' end with two crRNAs loaded onto two
199 separate RNPs and the two independent libraries combined on one flow cell (Supp. Fig. 1iii).

200

201 **Nanopore sequencing and data analysis**

202 Cas9 targeted long-read libraries were run on R9.4.1 flow cells on a minION Mk 1B following
203 manufacturer's instructions for Cas9 sequencing kit (SQK-CS9109) (www.nanoporetech.com).
204 Reads were converted from fast5 to fastq with guppy (v4.2.2) on MinKNOW (v20.10.3)
205 MinKNOW Core (v4.1.2) with fast base-calling option for the base-call model and minimum Q-
206 score of 7 option for read filtering. To analyze LRS results, guppy base-called fastq files were
207 imported into Qiagen CLC Genomics Workbench (www.qiagen.com). Reference sequences
208 specific to each transgenic mouse line were obtained from NCBI nucleotide database
209 (www.ncbi.nlm.nih.gov/nucleotide/) and alignments generated using the Long-Read Support
210 (beta) plugin available in Qiagen CLC Genomics Workbench (www.digitalinsights.qiagen.com),
211 which utilizes components of open-source tool minimap2 (24). Default parameters for the long-
212 read alignment plugin were used. Aligned informative long-reads were extracted and manually
213 queried against NCBI nr/nt and refseq genome databases
214 (<https://blast.ncbi.nlm.nih.gov/Blast.cgi>) and UCSC genome browser with BLAT tool
215 (<https://genome.ucsc.edu>). Graphical output obtained from CLC Genomics Workbench and
216 GraphPad (www.graphpad.com) were amended with Adobe Illustrator (www.adobe.com)
217 (Adobe Systems, San Jose, CA, USA) for illustration purposes.

218

219 **Genotyping and transgene copy number analysis**

220 Small ear biopsies were taken before weaning and gDNA was extracted using Qiagen DNeasy
221 Blood & Tissue Kit (cat#69504) following manufacturer's instructions (www.qiagen.com).
222 Progeny of (+/tg) x (+/tg) heterozygous crosses were assessed for CRISPR-LRS mapped
223 integration loci of the transgene. For genotyping, PCR conditions were the following: step 1, 95
224 °C for 3 min; step 2, 95 °C for 30 sec, 58 °C for 30 sec, and 72 °C for 1 min for 35 cycles; step
225 3, 72 °C for 10 min. Sequences for all genotyping amplicons were confirmed by Sanger
226 sequencing (Supp. Table I). For transgene copy number determination, gDNA was diluted to
227 50ng for input. For the BAC mouse lines, two primer sets to the *chloramphenicol resistance*

228 *gene* served as proxy for the BAC transgene, where values were normalized to an internal
229 control locus (Supp. Table 1) (1, 2, 9). For the *Cre*-driver mouse line, two primer sets to *Cre*
230 were normalized to same internal control locus used for the BAC mouse lines. The *Itga8*-
231 *CreER^{T2}* mouse, known to have one copy of *Cre* (manuscript in preparation), served as a
232 calibrator for one copy of *Cre*. Real time quantitative PCR conditions were the following: step1,
233 95 °C for 3 min; step 2, 95 °C for 30sec, 60 °C for 30 sec, and 72 °C for 30 sec for 40 cycles.

234

235 **Data availability**

236 Data generated by ONT LRS have been submitted to NCBI SRA database
237 (www.ncbi.nlm.nih.gov/sra) under BioProject number PRJNA759232 and will be publically
238 available after manuscript acceptance.

239

240

241 **Declarations**

242 **Ethics approval and consent to participate**

243 Not applicable

244

245 **Consent for publication**

246 Not applicable

247

248 **Availability of data and materials**

249 Nanopore long read sequencing data are available at NCBI Sequence Read Archive (SRA)
250 under accession number PRJNA759232.

251

252 **Competing interests**

253 The authors declare no competing interests

254

255 **Funding**

256 Work was supported by grants HL138987 and HL147476 to J.M.M. and HL122686 and
257 HL139794 to X.L.

258

259 **Author contributions**

260 W.B.B. and J.M.M designed the study.

261 A.Y., S.G. and WZ maintained mouse colonies.

262 W.B.B. performed the experiments.

263 W.B.B. and J.M.M. analyzed and interpreted data

264 X.L. provided liver tissue.

265 W.B.B. and J.M.M. wrote the paper.

266 All authors read and approved the final manuscript.

267

268 **Acknowledgements**

269 We wish to thank Akelia Wauchope-Odumbo and Carl Woodham at Oxford Nanopore
270 Technologies (ONT) for their combined help with use of long-read nanopore
271 sequencing.

272

273

274 **References**

275

276 1. Goodwin LO, Splinter E, Davis TL, Urban R, He H, Braun RE, et al. Large-scale
277 discovery of mouse transgenic integration sites reveals frequent structural variation and
278 insertional mutagenesis. *Genome Res.* 2019;29(3):494-505.

279 2. Nicholls PK, Bellott DW, Cho TJ, Pyntikova T, Page DC. Locating and
280 Characterizing a Transgene Integration Site by Nanopore Sequencing. *G3 (Bethesda).*
281 2019;9(5):1481-6.

282 3. Nakanishi T, Kuroiwa A, Yamada S, Isotani A, Yamashita A, Tairaka A, et al.
283 FISH analysis of 142 EGFP transgene integration sites into the mouse genome.
284 *Genomics.* 2002;80(6):564-74.

285 4. Dubose AJ, Lichtenstein ST, Narisu N, Bonnycastle LL, Swift AJ, Chines PS, et
286 al. Use of microarray hybrid capture and next-generation sequencing to identify the
287 anatomy of a transgene. *Nucleic Acids Res.* 2013;41(6):e70.

288 5. Cain-Hom C, Splinter E, van Min M, Simonis M, van de Heijning M, Martinez M,
289 et al. Efficient mapping of transgene integration sites and local structural changes in *Cre*
290 transgenic mice using targeted locus amplification. *Nucleic Acids Res.* 2017;45(8):e62.

291 6. Schmidt M, Schwarzwaelder K, Bartholomae C, Zaoui K, Ball C, Pilz I, et al.
292 High-resolution insertion-site analysis by linear amplification-mediated PCR (LAM-
293 PCR). *Nat Methods.* 2007;4(12):1051-7.

294 7. de Vree PJ, de Wit E, Yilmaz M, van de Heijning M, Klous P, Verstegen MJ, et al.
295 Targeted sequencing by proximity ligation for comprehensive variant detection and local
296 haplotyping. *Nat Biotechnol.* 2014;32(10):1019-25.

297 8. Liang Z, Breman AM, Grimes BR, Rosen ED. Identifying and genotyping
298 transgene integration loci. *Transgenic Res.* 2008;17(5):979-83.

299 9. Sailer S, Coassin S, Lackner K, Fischer C, McNeill E, Streiter G, et al. When the
300 genome bluffs: a tandem duplication event during generation of a novel Agmo knockout
301 mouse model fools routine genotyping. *Cell Biosci.* 2021;11(1):54.

302 10. Jinek M, Chylinski K, Fonfara I, Hauer M, Doudna JA, Charpentier E. A
303 programmable dual-RNA-guided DNA endonuclease in adaptive bacterial immunity.
304 *Science.* 2012;337(6096):816-21.

305 11. Deamer D, Akeson M, Branton D. Three decades of nanopore sequencing. *Nat*
306 *Biotechnol.* 2016;34(5):518-24.

307 12. Kono N, Arakawa K. Nanopore sequencing: Review of potential applications in
308 functional genomics. *Dev Growth Differ.* 2019;61(5):316-26.

309 13. Wongsurawat T, Jenjaroenpun P, De Loose A, Alkam D, Ussery DW, Nookaew I,
310 et al. A novel Cas9-targeted long-read assay for simultaneous detection of IDH1/2
311 mutations and clinically relevant MGMT methylation in fresh biopsies of diffuse glioma.
312 *Acta Neuropathol Commun.* 2020;8(1):87.

313 14. Walsh T, Casadei S, Munson KM, Eng M, Mandell JB, Gulsuner S, et al.
314 CRISPR-Cas9/long-read sequencing approach to identify cryptic mutations in BRCA1
315 and other tumour suppressor genes. *J Med Genet.* 2020.

316 15. Miyamoto S, Aoto K, Hiraide T, Nakashima M, Takabayashi S, Saitsu H.
317 Nanopore sequencing reveals a structural alteration of mirror-image duplicated genes in
318 a genome-editing mouse line. *Congenit Anom (Kyoto).* 2020;60(4):120-5.

- 319 16. Watson CM, Crinnion LA, Hewitt S, Bates J, Robinson R, Carr IM, et al. Cas9-
320 based enrichment and single-molecule sequencing for precise characterization of
321 genomic duplications. *Lab Invest.* 2020;100(1):135-46.
- 322 17. van Haasteren J, Munis AM, Gill DR, Hyde SC. Genome-wide integration site
323 detection using Cas9 enriched amplification-free long-range sequencing. *Nucleic Acids*
324 *Res.* 2021;49(3):e16.
- 325 18. Gabrieli T, Sharim H, Fridman D, Arbib N, Michaeli Y, Ebenstein Y. Selective
326 nanopore sequencing of human BRCA1 by Cas9-assisted targeting of chromosome
327 segments (CATCH). *Nucleic Acids Res.* 2018;46(14):e87.
- 328 19. McDonald TL, Zhou W, Castro CP, Mumm C, Switzenberg JA, Mills RE, et al.
329 Cas9 targeted enrichment of mobile elements using nanopore sequencing. *Nat*
330 *Commun.* 2021;12(1):3586.
- 331 20. Gilpatrick T, Lee I, Graham JE, Raimondeau E, Bowen R, Heron A, et al.
332 Targeted nanopore sequencing with Cas9-guided adapter ligation. *Nat Biotechnol.*
333 2020;38(4):433-8.
- 334 21. Lyu Q, Xu S, Lyu Y, Choi M, Christie CK, Slivano OJ, et al. SENCER stabilizes
335 vascular endothelial cell adherens junctions through interaction with CKAP4. *Proc Natl*
336 *Acad Sci U S A.* 2019;116(2):546-55.
- 337 22. Burgio G, Teboul L. Anticipating and Identifying Collateral Damage in Genome
338 Editing. *Trends Genet.* 2020;36(12):905-14.
- 339 23. Miano JM, Ramanan N, Georger MA, de Mesy Bentley KL, Emerson RL, Balza
340 RO, Jr., et al. Restricted inactivation of serum response factor to the cardiovascular
341 system. *Proc Natl Acad Sci U S A.* 2004;101(49):17132-7.
- 342 24. Li H. Minimap2: pairwise alignment for nucleotide sequences. *Bioinformatics.*
343 2018;34(18):3094-100.
- 344 25. Labun K, Montague TG, Krause M, Torres Cleuren YN, Tjeldnes H, Valen E.
345 CHOPCHOP v3: expanding the CRISPR web toolbox beyond genome editing. *Nucleic*
346 *Acids Res.* 2019;47(W1):W171-W4.
- 347
- 348

349 **Figure Legends**

350

351 **Figure 1. CRISPR-LRS mapping of RP11-744N12 BAC to chromosome 15 in mouse**

352 **genome.** (A) Dashed red line represents integration locus of RP11-744N12 BAC within first
353 intron of *Egflam* on chromosome 15, section qA1. Blue and yellow arrows represent the 5' and
354 3' end crRNAs, respectively, used to make Targeted-CRISPR-LRS libraries (see Supp. Fig1i
355 flow chart). (i) Histograms for informative reads from Targeted-CRISPR-LRS libraries at either 5'
356 or 3' end of the RP11-744N12 BAC. (ii) Black triangles represent flanking tandem crRNAs used
357 to make Enrichment-CRISPR-LRS libraries to interrogate 5' and 3' ends of the RP11-744N12
358 integration locus on chromosome 15, section qA1. (iii) Sanger sequencing verification of
359 CRISPR-LRS mapped RP11-744N12 integration locus for 5' and 3' ends of the RP11-744N12
360 integration locus. (B) PCR genotyping of mice progeny from (+/tg) x (+/tg) cross with primer
361 schematics. Primer pair A+B interrogated the breakpoint junction of RP11-744N12 BAC and
362 chromosome 15, section qA1. Primer pair A+C interrogated wild type integration locus. To
363 check for presence of RP11-744N12 BAC transgene, internal primer pairs D+E and F+G
364 targeted 5' and 3' regions of the RP11-744N12 BAC sequence, respectively.

365

366 **Figure 2. CRISPR-LRS mapping of *Sm22Cre*-driver to chromosome 14 in mouse genome.**

367 (A) Dashed red line represents integration locus of *Sm22Cre*-driver within chromosome 14,
368 section qE2.1. Informative long reads were compiled to build an integration locus map. Dashed
369 black line box represents *Sm22Cre*-driver integration locus. Blue and yellow arrows represent
370 internal overlapping 5' and 3' end crRNAs used to make a Targeted-CRISPR-LRS library (see
371 Supp. Fig 1iii flow chart). (i) Histogram for informative reads from the Targeted-CRISPR-LRS
372 library. (ii) Sanger sequencing verification of CRISPR-LRS mapped *Sm22Cre*-driver integration
373 locus, represented by dashed black line box highlighted in (A). (iii) qPCR determination of
374 transgene copy number with (+/tg) and (tg/tg) pups with approximately 20 and 40 copies,
375 respectively. Data normalized to internal control locus and calibrator (*Itga8-CreER^{T2}*, see
376 Methods for details). $N = 2$ for calibrator (*Itga8-CreER^{T2}*), $N = 4$ for *Sm22Cre* (+/tg) and (tg/tg).
377 Values graphed as mean \pm SD. (B) PCR genotyping of mice progeny from (+/tg) x (+/tg) cross
378 with primer schematics. Primer pair A+B interrogated the breakpoint junction of *Sm22Cre*-driver
379 and chromosome 14, section qE2.1, represented by dashed black line box highlighted in (A).
380 Primer pair A+C interrogated wild type integration locus. To check for presence of transgene,
381 internal primer pair D+E targeted the *Cre* transgene.

382

383 **Supplemental Figure 1. CRISPR-LRS flow chart.**

384 Overview of library preparation for Targeted- (i-iii) and Enrichment- (iv) CRISPR-LRS libraries.

385

386 **Supplemental Figure 2. CRISPR-LRS determination of tandem BAC integration for two**

387 **BAC mouse lines.** Overview of Targeted-CRISPR-LRS sequencing illustrating tandem

388 integration of BAC sequence for (A) CTD-2518N7 and (B) RP11-997L11 BAC mouse lines (See

389 Supp. Fig1ii flow chart).

390

391 **Supplemental Figure 3. Relative transgene copy number for BAC and Cre-driver mouse**

392 **lines.** qPCR to determine transgene copy number, normalized to internal control locus. (A) Two

393 primer sets (i and ii) targeting *chloramphenicol resistance gene*, common gene found in BAC

394 cloning vectors. For RP11-744N12 mouse line, (+/tg) and (tg/tg) pups demonstrated one and

395 two copies, respectively. For both CTD-2518N7 and RP11-997L11 mouse lines, (+/tg) pups

396 demonstrated approximately 3 copies. (B) Two primer sets (i and ii) targeting *Cre* sequence.

397 *Itga8-CreER^{T2}* mouse served as calibrator for one copy of *Cre*, serving as (+/tg) control. For

398 *Sm22Cre*-driver mouse line, (+/tg) and (tg/tg) pups demonstrated approximately 20 and 40

399 copies, respectively. $n = 9$ for RP11-744N12 (+/tg), $n = 7$ for RP11-744N12 (tg/tg), $n = 6$ for

400 CTD-2518N7 (+/tg), $n = 3$ for RP11-997L11 (+/tg), $n = 2$ for *Itga8-CreER^{T2}*, $n = 4$ for both

401 *Sm22Cre* (+/tg) and (tg/tg). Values graphed as mean \pm SD.

402

403 **Supplemental Table 1. crRNAs and primers used for CRISPR-LRS**

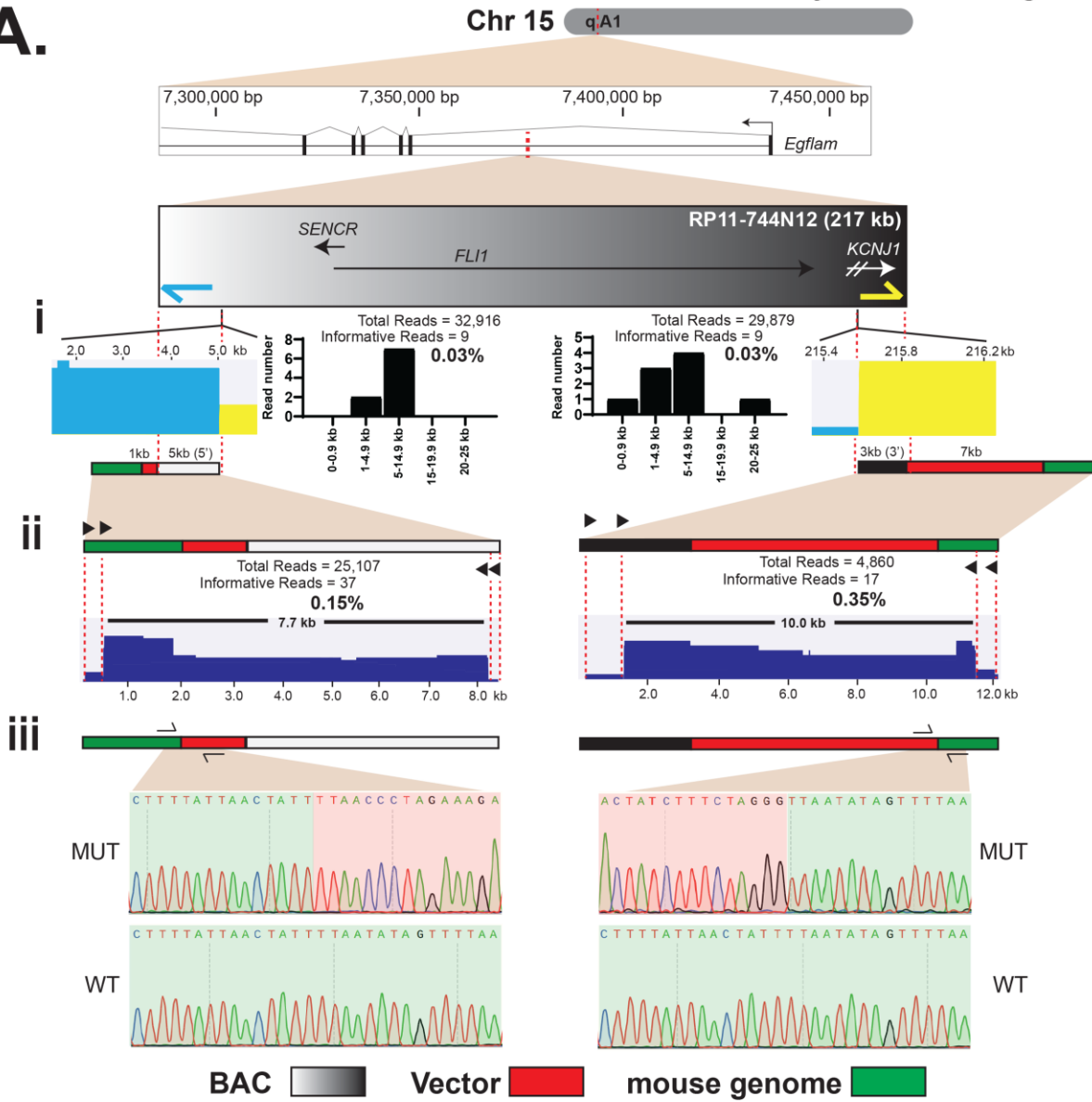
404

405 **Supplemental Table 2. Nanopore long-read library metrics for CRISPR-LRS**

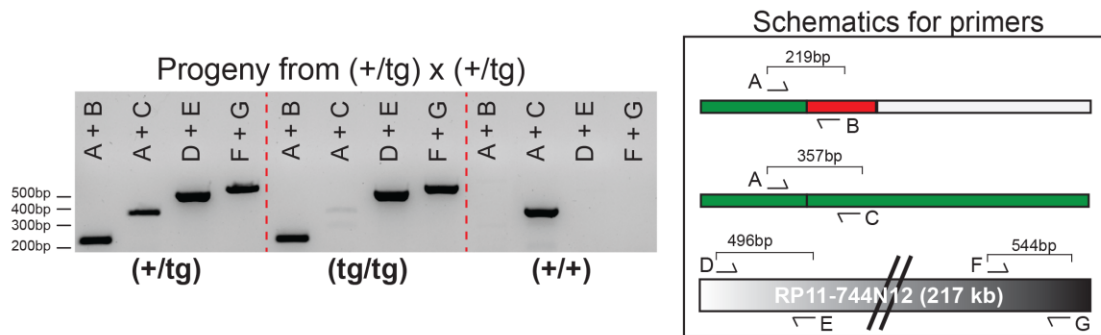
406

Bryant et. al, Figure 1

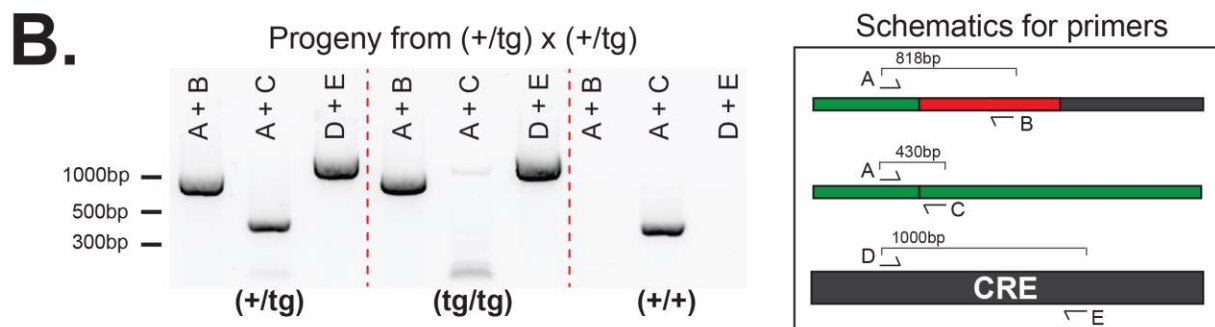
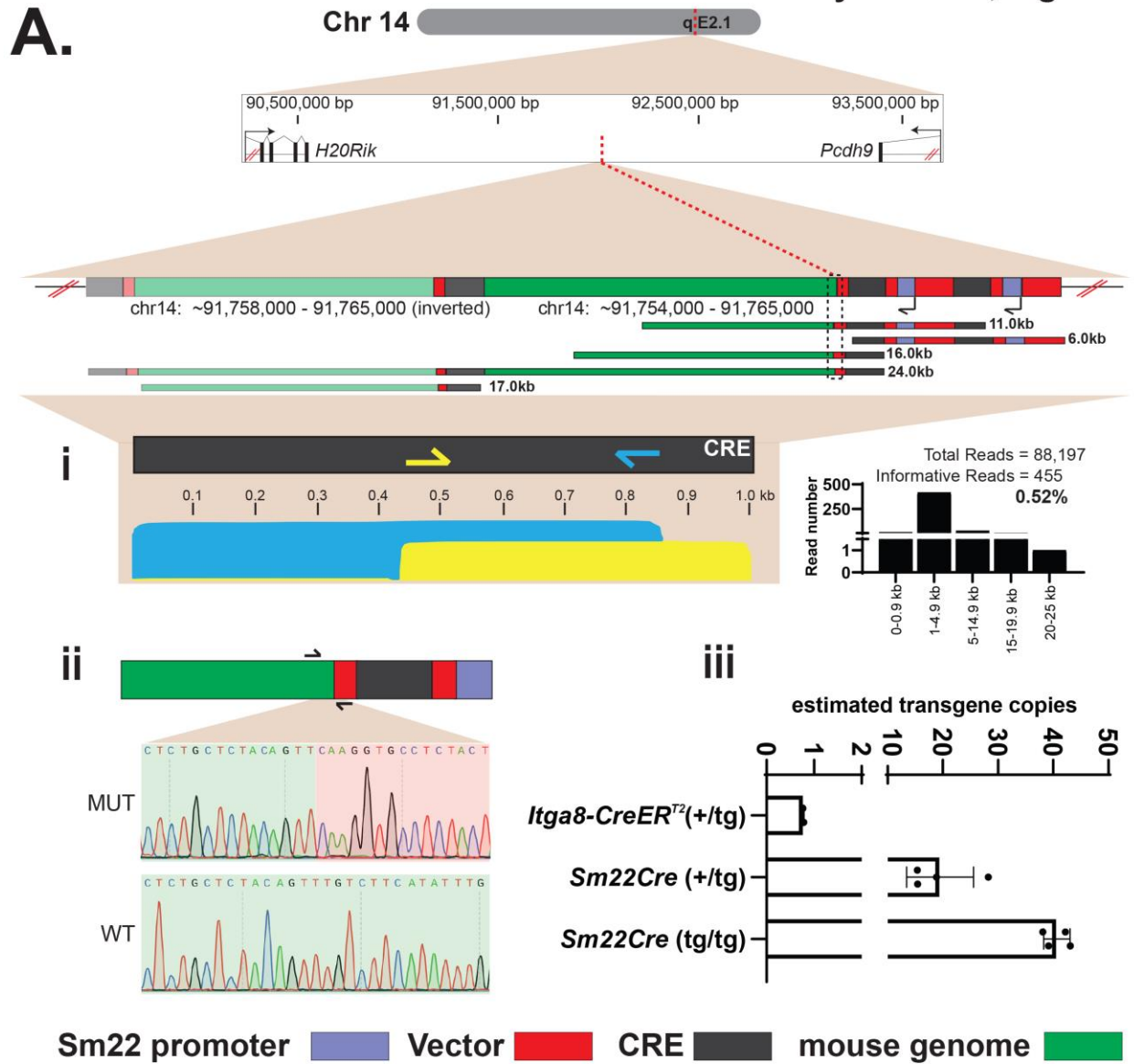
A.



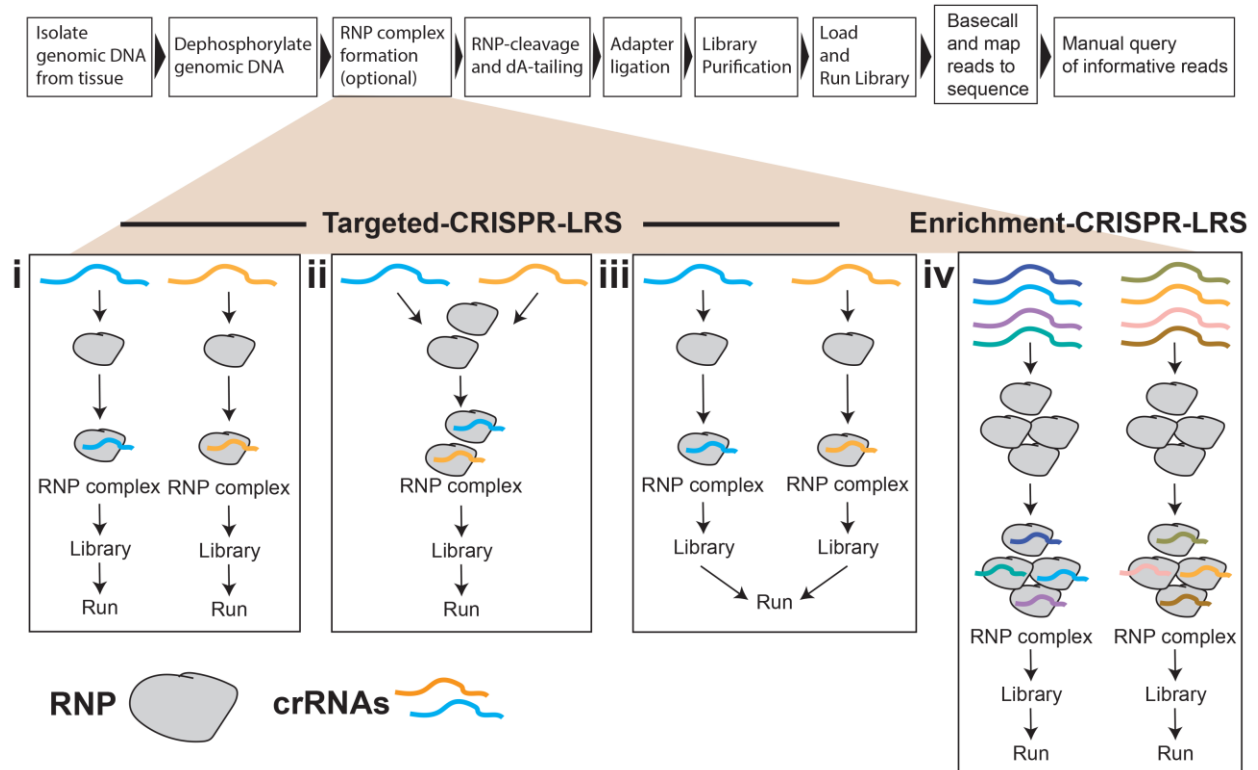
B.



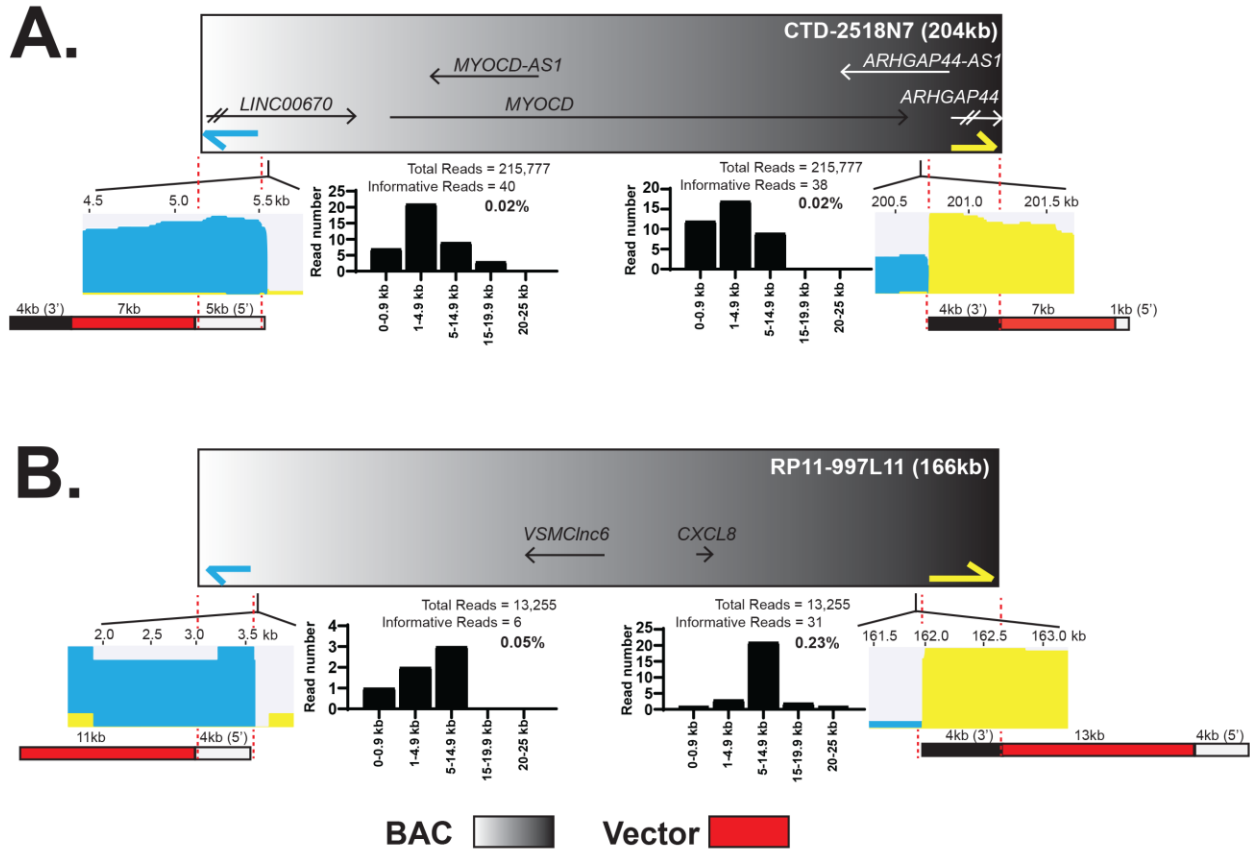
Bryant et. al, Figure 2



Bryant et. al, Supp. Figure 1

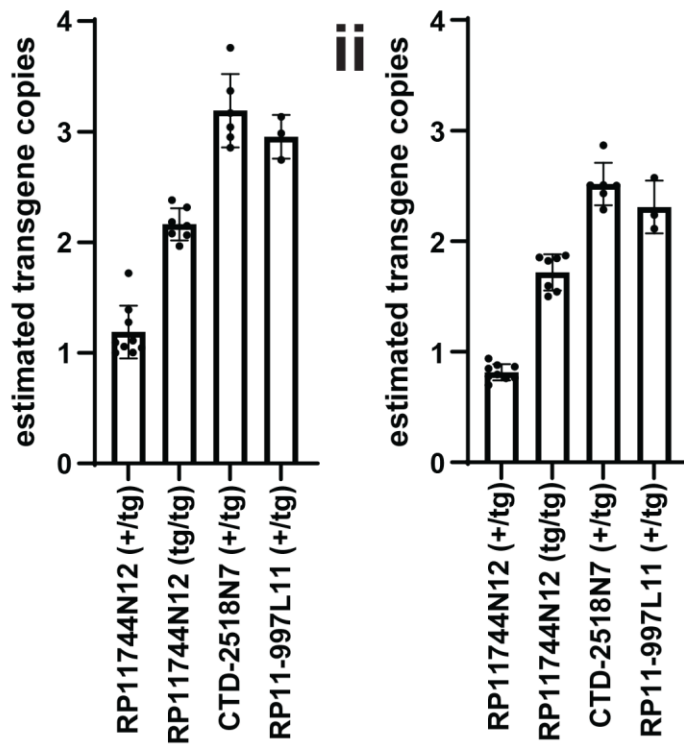


Bryant et. al, Supp. Figure 2



Bryant et. al, Supp. Figure 3

A.



B.

